Relaxation properties in a lattice gas model with asymmetrical particles

2002 J. Phys. A: Math. Gen. 35 3359

(http://iopscience.iop.org/0305-4470/35/15/301)

INSTITUTE OF PHYSICS PUBLISHING JOURNAL OF PHYSICS A: MATHEMATICAL AND GENERAL

J. Phys. A: Math. Gen. **35** (2002) 3359–3368 PII: S0305-4470(02)26283-6

Relaxation properties in a lattice gas model with asymmetrical particles

A Díaz-Sánchez[1,2,3], Antonio de Candia[1,2] and Antonio Coniglio[1,2]

[1] Dipartimento di Scienze Fisiche, Università di Napoli 'Federico II', Complesso Universitario di Monte Sant'Angelo, Via Cintia, I-80126 Napoli, Italy
[2] INFM, Unità di Napoli, Napoli, Italy
[3] Departamento de Física Aplicada, Universidad Politécnica de Cartagena, Campus Muralla del Mar, Cartagena, E-30202 Murcia, Spain

E-mail: andiaz@upct.es

Received 27 June 2001, in final form 1 February 2002
Published 5 April 2002
Online at stacks.iop.org/JPhysA/35/3359

Abstract

We study the relaxation process in a two-dimensional lattice gas model, where the interactions originate from the excluded volume. In this model particles have three arms with an asymmetrical shape, which results in geometrical frustration that inhibits full packing. Relaxation functions are well fitted at long times by a stretched exponential form, with a β exponent decreasing when the density is raised until the percolation transition is reached, and constant for higher densities. The structural arrest of the model seems to happen only at the maximum density of the model, where both the inverse diffusivity and the relaxation times diverge with a power law. The dynamical non-linear susceptibility, defined as the fluctuations of the self-overlap autocorrelation, exhibits a peak at some characteristic time, which also seems to diverge at the maximum density.

PACS numbers: 64.70.Pm, 05.50.+q, 75.10.−b

1. Introduction

Most glassy systems, such as structural glasses, ionic conductors, supercooled liquids, polymers, colloids and spin glasses [1], have similar complex dynamical behaviour. As the temperature is lowered the relaxation times increase drastically, and the relaxation functions deviate strongly from a single-exponential function at some temperature T^* well above the dynamical transition. In the long-time regime they can be well fitted by a stretched exponential or Kohlrausch–Williams–Watts [2] function

$$\phi(t) \propto \exp[-(t/\tau)^{\beta}] \tag{1}$$

with $0 < \beta < 1$. There are two mechanisms driving non-exponential relaxation. In a disordered model such as spin glasses, it is caused by the existence of non-frustrated ferromagnetic-type clusters of interactions [3], and therefore is a direct consequence of the quenched disorder [4]. Another mechanism in frustrated systems is based on the percolation transition of the Kasteleyn–Fortuin and Coniglio–Klein cluster [5]. In this approach disorder is not needed to obtain non-exponential relaxation [6].

In spin glasses there is a thermodynamic transition at a defined temperature T_{SG}, where the non-linear susceptibility and the static correlation length diverge. In glass forming liquids it seems that there is no sharp thermodynamic transition, and no diverging static length. However, numerical studies have identified long-lived dynamical structures which are characterized by a typical length and a typical relaxation time, which depend on temperature and density [7]. In order to characterize this behaviour a dynamical non-linear susceptibility was introduced by Donati *et al* [8], both for spin models and for structural glasses. They have found that the dynamical susceptibility exhibits a maximum at some characteristic time which diverges as the dynamical transition temperature is approached from above. In the annealed version of the frustrated Ising lattice gas model [9] a similar behaviour has been found, while in the quenched version the dynamical susceptibility is always increasing, due to the presence of the thermodynamic transition [10].

Our understanding of the macroscopic process of relaxation in structural glasses, starting from the microscopic motion of the particles, has been attained using different microscopic models, for example the hard-square model [11], the kinetically constrained models [12,13] and the frustrated Ising lattice gas (FILG) model [14]. These models have reproduced some aspects of the glassy phenomenology, and recently the FILG model has been studied in its quenched and annealed versions with kinetic constraints [10]. The results found in the annealed version seems to be closer to the experimental ones. In this paper we consider a two-dimensional geometrical model, which contains as main ingredients only geometrical frustration without quenched disorder and without kinetic constraints, as quenched disorder is not appropriate to study structural glasses and kinetic constraints are somewhat artificial. Similar models have already been proposed [9, 15] and applied to study granular material [16].

In section 2 we present the model and in section 3 we study its percolation properties. In section 4 we show the dynamical results, and finally in section 5 we present our conclusions.

2. The model

In this paper we introduce a model which can be considered as an illustration of the concept of frustration arising as a packing problem. In systems without underlying crystalline order, frustration is typically generated by the geometrical shape of the molecules, which prevents the formation of close-packed configurations at low temperature or high density; for systems with underlying crystalline order, frustration arises when the local arrangement of molecules kinetically prevents all the molecules from reaching the crystalline state.

An example of a glass-former that has difficulty in achieving crystalline order is *ortho*-terphenyl, whose molecule is made of three rings. This system can be loosely modelled with a simple lattice model, in which 'T'-shaped objects occupy the vertices of a square lattice with one of four possible orientations.

Assuming that the arms cannot overlap due to excluded volume, we see that only for some relative orientations can two particles occupy nearest-neighbour vertices. Consequently, depending on the local arrangement of particles, there are sites on the lattice that cannot be occupied (see figure 1). This type of 'packing' frustration thus induces defects or holes in the system. This model resembles the hard-square lattice gas model [11], which can be seen as

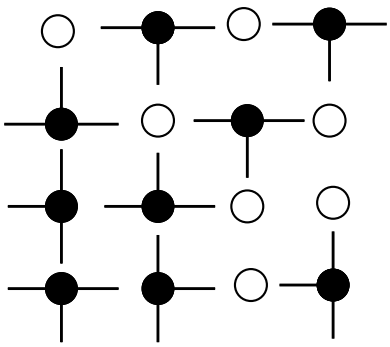

Figure 1. Schematic picture of one particular configuration in a system size of 4^2 and density $\rho = 9/16$.

'+'-shaped objects on the vertices of a square lattice with excluded volume interaction. A very important difference between these two models is the internal degree of freedom due to the particle shape, which is absent from the latter.

We consider a two-dimensional square lattice and impose periodic boundary conditions. In our system the maximum of density is $\rho_{\max} = 2/3$, at which all possible bonds are occupied by an arm. A configuration of density $\rho_{\max}$ is a ground state of the system, corresponding to chemical potential $\mu \to \infty$. This can be obtained for any size, constructing larger systems from smaller ones with $\rho_{\max}$ and appropriated boundary conditions. In this way one can build an extensive number of different ground states that lack spatial order.

We have simulated the diffusion and rotation dynamics of this model by Monte Carlo methods. The dynamics of the particles is given by the following algorithm:

(i) pick a particle at random;
(ii) pick a site at random between the four nearest-neighbour ones;
(iii) choose randomly an orientation of the particle;
(iv) if it does not cause the overlapping of two arms, move the particle into the given site with the given orientation;
(v) if the diffusion movement is not possible, choose a random orientation and try to rotate the particle to this new orientation;
(vi) advance the clock by $1/N_s$, where N_s is the number of sites, and go to (i).

Studying the dynamics by Monte Carlo simulations, the finite-size effects are larger when we are near to $\rho_{\max}$, because the particles can be enclosed in cages, and the diffusion is blocked. In lattices of finite size, cages may be indefinitely stable. This has also been observed in the hard-square lattice gas model [11], where at the maximum of density the particles are on the diagonals, but in lattices of finite size indefinitely stable cages of particles are formed at lower densities.

3. Percolation transition

In order to investigate whether the percolation transition has effects on the dynamics, in this section we analyse the percolation properties of the model, and relate the percolation density to a change in the dynamical properties of the model. The particles have three arms, and there are two bonds per site on the lattice, so the density of bonds occupied by an arm is given by $\sigma = 3\rho/2$, where ρ is the density of particles. Therefore, if the correlations of the arms were

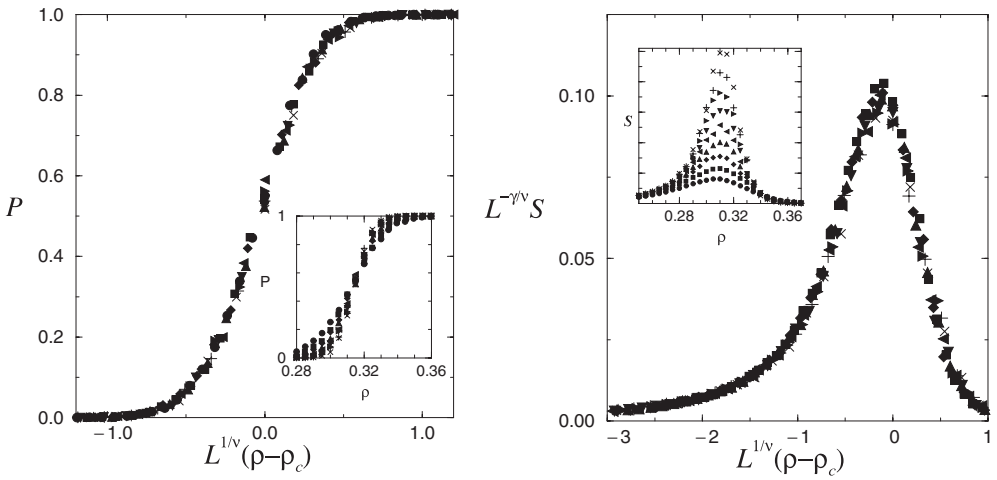

Figure 2. Finite-size scaling of (*a*) $P(\rho)$ and (*b*) $S(\rho)$ for lattice sizes $L = 40$, 50, 60, 70, 80, 90, 100, 110 and 120. Inset: (*a*) $P(\rho)$ and (*b*) $S(\rho)$ for the same sizes.

not important, the arm percolation would occur at the density $\sigma_c = 1/2$, corresponding to $\rho_c = 1/3$. Nevertheless we expect some correlation effects.

We have simulated our system for various lattice sizes around the percolation density in order to determine ρ_c. For each density we have reached equilibrium and then, taking 10^4 steps, we have evaluated the probability of existence of a spanning cluster P and the mean cluster size $S = \sum_s s^2 n_s$, where n_s is the density of finite clusters of size s.

Around the percolation density the averaged quantities $P(\rho)$ and $S(\rho)$, for different values of the lattice size L, should obey the finite-size scaling [17]

$$P(\rho) = F_P[L^{1/\nu}(\rho - \rho_c)] \tag{2}$$

$$S(\rho) = L^{\gamma/\nu} F_S[L^{1/\nu}(\rho - \rho_c)] \tag{3}$$

where γ and ν are then critical exponents, and $F_P(x)$ and $F_S(x)$ are universal functions of a non-dimensional quantity x. Figure 2 shows the finite-size scaling of P and S. We have selected the values of the exponent corresponding to the two-dimensional site–bond percolation universality class [17], that is $\nu = 4/3$ and $\gamma = 43/18$, and we have found $\rho_c = 0.315 \pm 0.003$. The critical density can also be determined from $P(\rho)$ as the density at which curves corresponding to different sizes cross. From the inset of figure 2(*a*) we see that ρ_c is between 0.315 and 0.32, so the arm correlations and the thermal process decrease the critical density with respect to the random bond problem.

4. Dynamical results

To make a link with the spin-glass theory, where one studies relaxation functions in the form of the 'self-overlap' $\langle S_i(t) S_i(t') \rangle$, we wish now to define a self-overlap parameter for our model. Different definitions of q can be used, and the form of the relaxation functions is different for different overlap parameters. Here we define a self-overlap parameter similar to that defined in [8] for liquids, but which also takes into account the orientation of the particles, besides their position. The orientation of the particle is defined by the discrete values of the angle, $\phi_i = 0, \pi/2, \pi$ or $3\pi/2$, and we define the self-overlap as

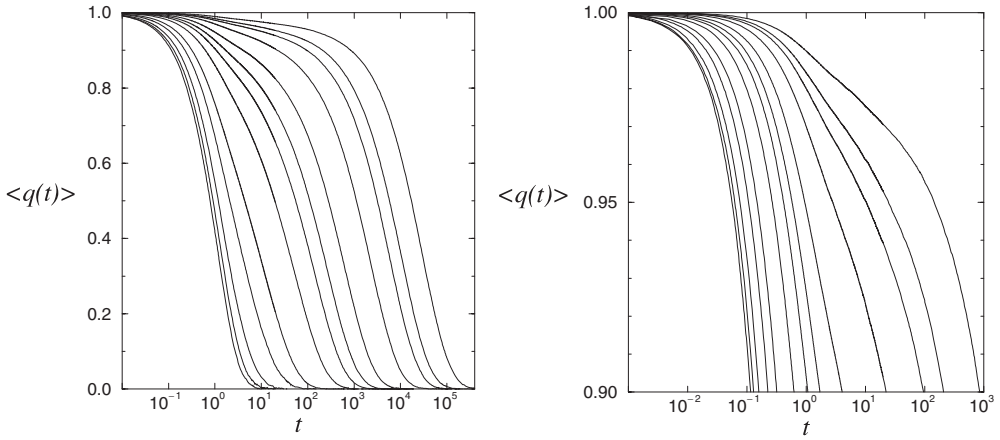

Figure 3. (*a*) Relaxation functions of the self-overlap for system size 64^2 and densities $\rho = 0.2$, 0.3, 0.4, 0.5, 0.55, 0.6, 0.62, 0.63, 0.64, 0.65, 0.655, 0.657 and 0.66. (*b*) Zoom of the range 0.9–1.0, where one can see the presence of two distinct steps in the relaxation of the self-overlap.

$$\langle q(t)\rangle = \frac{1}{N\rho}\sum_i \langle n_i(t')n_i(t'+t)\cos[\phi_i(t'+t)-\phi_i(t')]\rangle \tag{4}$$

where $n_i(t) = 0, 1$ is the occupation number of site i at time t, $\phi_i(t)$ the orientation of the particle on site i at time t, N the number of sites and $\langle\cdots\rangle$ the average with respect to the reference time t'. This parameter is a generalization of the self-overlap defined in [10], where the orientation ϕ_i plays the role of the spin variables. At time $t = 0$, the self-overlap is $\langle q(0)\rangle = 1$, and goes to zero for $t \to \infty$ in the liquid phase. The glassy phase is signalled by the fact that $\langle q(t)\rangle$ tends for $t \to \infty$ to a value greater than zero.

In figure 3(*a*) we show the relaxation function of the self-overlap parameter, for a system of size 64^2 and densities between $\rho = 0.2$ and 0.66. Each curve is obtained by averaging over a time interval for t' of 10^4–10^8 Monte Carlo steps, depending on the density. At the highest densities we start to observe two steps in the relaxation functions (see figure 3(*b*)), which suggest that two different timescales are beginning to decouple in the system. The first shorter timescale of the relaxation functions is due to the rotations of the particles in a frozen environment, which appears as quenched on this timescale, while the second longer timescale is due to the evolution of the environment and final relaxation to equilibrium. Indeed, we shall see that the density–density autocorrelation functions, which do not depend on rotational degrees of freedom, always show a single relaxation time.

We have then compared the relaxation functions $\langle q(t)\rangle$ with the predictions that the mode-coupling theory (MCT) of supercooled liquids makes for the relaxation functions of supercooled liquids [18], that we now report briefly. The theory makes distinct predictions for two different timescales, called t_σ and τ_α, which both diverge at the transition T_c, but with different exponents, $t_\sigma \propto |T - T_c|^{-1/2a}$ and $\tau_\alpha \propto |T - T_c|^{-\gamma}$, with

$$\gamma = \frac{1}{2a} + \frac{1}{2b}, \tag{5}$$

so τ_α/t_σ also diverges. The critical exponents a and b are not independent, but are related to the so-called exponent parameter λ by the equations

$$\frac{\Gamma^2(1-a)}{\Gamma(1-2a)} = \frac{\Gamma^2(1+b)}{\Gamma(1+2b)} = \lambda. \tag{6}$$

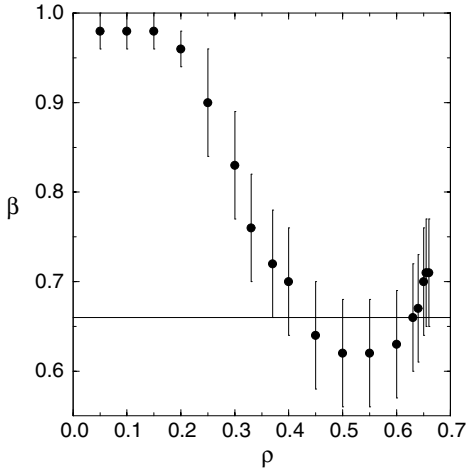

Figure 4. Parameter β of the stretched exponential for the self-overlap relaxation functions, for the same system size and densities as figure 3. The solid line corresponds to $\beta = 0.66$.

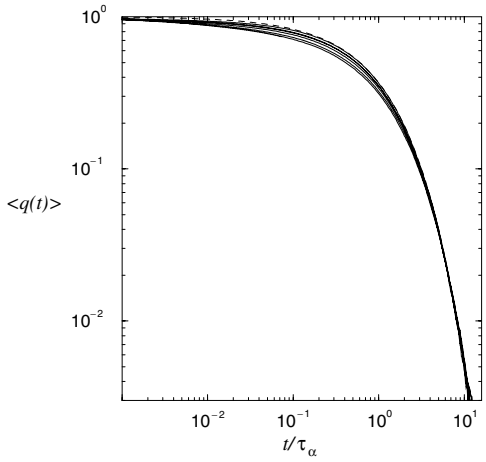

Figure 5. Time–density superposition principle for the relaxation function of the self-overlap, for densities $\rho =$ 0.62, 0.63, 0.64, 0.65, 0.655, 0.657 and 0.66. The dashed curve is a stretched exponential with exponent $\beta = 0.71$.

Near the transition, and in the intermediate timescale $t_0 \ll t \ll \tau_\alpha$, where t_0 is a microscopic time, the theory predicts that the relaxation functions can be fitted by

$$\phi(t) = f + hc_\sigma g_\pm(t/t_\sigma), \tag{7}$$

where f and h are constants, $c_\sigma = |\sigma|^{1/2}$ is the so-called critical amplitude and $t_\sigma = |\sigma|^{-1/2a}$. The parameter σ, called the separation parameter, plays the role of $T_c - T$, being negative in the liquid phase, and positive in the glassy phase. The universal function $g_\pm(\hat{t})$, where $\pm$ refer respectively to the glassy and liquid phase, depends only on the exponent parameter λ. It has the limiting behaviour $g_\pm(\hat{t}) = \hat{t}^{-a}$ for $t_0/t_\sigma \ll \hat{t} \ll 1$, and $g_+(\hat{t}) = (1-\lambda)^{-1/2}$, $g_-(\hat{t}) = -B\hat{t}^b$ for $1 \ll \hat{t} \ll \tau_\alpha/t_\sigma$.

Furthermore, in the liquid phase $T > T_c$, the theory predicts that the relaxation functions can be fitted by a stretched exponential form (1) in the longest timescale, $t \gg \tau_\alpha$, where the exponent β is independent of the temperature. That means that, plotting the relaxation function $\phi(t)$ versus the rescaled time t/τ_α, the data should collapse on a single stretched exponential curve (time–temperature superposition principle).

We have compared the results obtained for the self-overlap relaxation functions with these predictions. For very low densities, $\rho < 0.1$, the relaxation function of the self-overlap $\langle q(t)\rangle$ of the model is well fitted by an exponential form. For $0.1 < \rho < 0.32$, we can fit the relaxation function with the stretched exponential form, with the exponent β decreasing slowly down to $\beta \approx 0.7$. For higher values of densities only the long-time tail of the relaxation functions is well fitted by a stretched exponential, with the exponent β depending very weakly on the density (constant within the errors) and ranging between $\beta = 0.64$ and 0.71. In figure 4 the exponent β is plotted as a function of the density. Note that $\rho = 0.32$ corresponds to the arm percolation of the model. Figure 5 shows the time–density superposition of the relaxation functions $\langle q(t)\rangle$, for densities between $\rho = 0.62$ and 0.66. Also shown as a dashed line is a stretched exponential function with an exponent $\beta = 0.71$. We then tried to fit the intermediate timescale of the self-overlap relaxation with the functional form (7). Recall that this fit is expected to be valid only in a time range $t_0 \ll t \ll \tau_\alpha$, where t_0 is a microscopic time, and τ_α is the timescale on which the function decays to zero. In figure 6 we show the result of the fit for densities

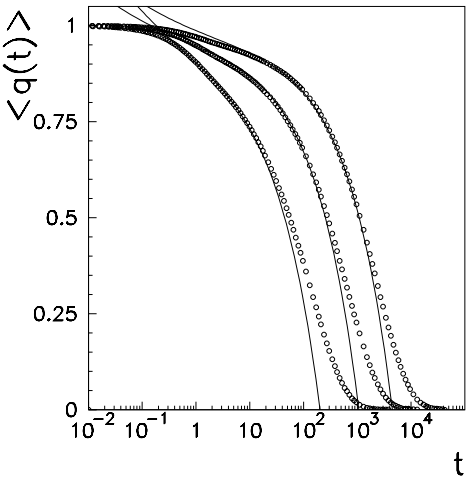

Figure 6. Fit of the intermediate time regime of the relaxation functions of the self-overlap, for densities $\rho = 0.62$, 0.64 and 0.65. The fitting function is $f + hc_\sigma g_\pm(t/t_\sigma)$ (dots), where the fitting parameters are λ, h, f and σ (see the text).

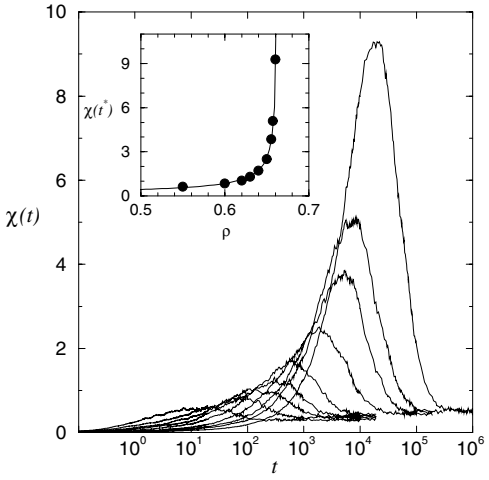

Figure 7. Dynamical susceptibility for size 64^2 and densities $\rho = 0.55$, 0.6, 0.62, 0.63, 0.64, 0.65, 0.655, 0.657 and 0.66. Inset: the maximum $\chi(t^*)$ as a function of density. The fitting function is a power law $\chi(t^*) = 0.12(0.664 - \rho)^{-0.7}$.

$\rho = 0.62$, 0.64 and 0.65, where the fitting parameters are λ, f, h and σ. The value of λ given from the fits is constant within the errors, and equal to $\lambda = 0.770 \pm 0.005$, which corresponds to exponents $a = 0.295 \pm 0.005$ and $b = 0.52 \pm 0.01$. Therefore, the relaxation functions $\langle q(t)\rangle$ agree quite well with the predictions of MCT of liquids.

We have also studied the behaviour of the dynamical non-linear susceptibility associated with the self-overlap parameter, which is defined as

$$\chi(t) = N[\langle q(t)^2\rangle - \langle q(t)\rangle^2]. \tag{8}$$

In figure 7 we show $\chi(t)$ for some values of the density. The maximum in the susceptibility $\chi(t^*)$ and the time of the maximum t^* seem to diverge together when the density grows. This has also been found previously in other models such as p-spin, Lennard-Jones binary mixture [8] and the annealed version of the FILG model [10]. In our model we obtain that the maximum of $\chi(t^*)$ can be fitted by the power law $\chi(t^*) \propto (\rho_{\max} - \rho)^{-\alpha}$. Here we have $\rho_{\max} = 0.664 \pm 0.002$ and $\alpha = 0.71 \pm 0.02$. The equilibrium value is $\chi(t \to \infty) = \rho^2/2$ for low densities and $\chi(t \to \infty) = 1/2$ for the higher ones.

The density–density autocorrelation function and its dependence on the time is an important property which characterizes the glassy behaviour. We have studied the self-part of the autocorrelation function of the density fluctuations, defined as

$$F_k^s(t) = \frac{1}{N}\sum_i \langle e^{i\boldsymbol{k}(\boldsymbol{r}_i(t'+t) - \boldsymbol{r}_i(t'))}\rangle, \tag{9}$$

where $\boldsymbol{r}_i(t)$ is the position of the ith particle in units of the lattice constant. The wavevector can take the values $\boldsymbol{k} = (2\pi/L)\boldsymbol{n}$, where $\boldsymbol{n}$ has integer components n_x and n_y ranging from 0 to $L/2$.

Figure 8 shows $F_k^s(t)$ corresponding to $k_x = \pi$ and $k_y = 0$ for different densities. For all densities the whole time interval of the autocorrelation function can be fitted by a stretched exponential function, $f(t) = \exp[-(t/\tau)^\beta]$, where the exponent β depends on the density. In figure 9 we show β as a function of the density. As happens for the relaxation of the self-overlap,

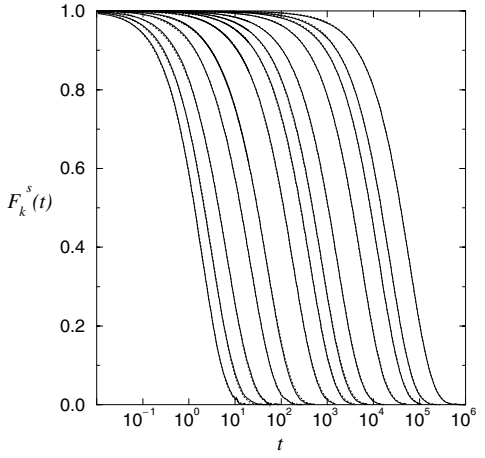

Figure 8. Self-part $F_{\boldsymbol{k}}^s(t)$ of the density–density autocorrelations for $k_x = \pi$ and $k_y = 0$, for the same system size and densities as figure 3. Dotted curves are fitting functions corresponding to stretched exponential functions.

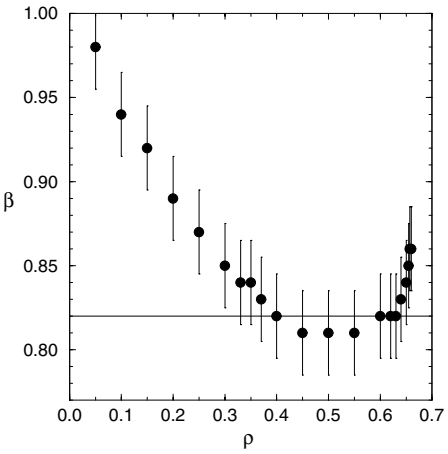

Figure 9. Parameter β of the stretched exponential for the function $F_{\boldsymbol{k}}^s(t)$, for densities $\rho = 0.05$, 0.1, 0.15, 0.2, 0.25, 0.3, 0.33, 0.35, 0.37, 0.4, 0.45, 0.5, 0.55, 0.6, 0.63, 0.64, 0.65, 0.655, 0.657 and 0.66. The solid line corresponds to $\beta = 0.82$.

the exponent β decreases with the density until a density near $\rho \approx 0.32$ is reached. Starting from this density, which corresponds to arm percolation, the exponent becomes constant, $\beta \approx 0.82$ (within the error bars), but with a different value of the exponent with respect to the self-overlap. At densities near to $\rho_{\max}$ the finite-size effects become important and β deviates from the constant value.

Different from what is observed in the relaxation of the self-overlap, the density–density autocorrelation functions do not show any evidence of the presence of two timescales. This depends on the fact that the functions $F_{\boldsymbol{k}}^s(t)$ take into account only the positions of the particles, and not their orientation. On the other hand the self-overlap relaxation $\langle q(t)\rangle$ takes into account both rotational and translational degrees of freedom, and shows a two-step decay for high densities.

The relaxation times τ_α, obtained from the fit of $F_{\boldsymbol{k}}^s(t)$ and $\langle q(t)\rangle$ with a stretched exponential function, are shown in figure 10. They can both be fitted by a power law $\tau \propto (\rho_{\max} - \rho)^{-\gamma}$, with $\gamma = 2.70 \pm 0.02$ and $\rho_{\max} = 0.666 \pm 0.003$, but with a different prefactor. Note that the value of γ coincides within the errors with that deduced by the exponents a and b given by the fit of figure 6, using the relation (5) predicted by MCT [18] which gives $\gamma = 2.65 \pm 0.05$.

We have calculated the diffusion coefficient from the mean-square displacement $\langle \Delta r(t)^2\rangle$ at very long times. The values obtained for D are well fitted by a power law near $\rho_{\max}$, $D \propto (\rho_{\max} - \rho)^\gamma$ with $\gamma = 2.70 \pm 0.02$ and $\rho_{\max} = 0.666 \pm 0.003$ (see the inset of figure 10). The power law agrees with the law found in some lattice gas models (the kinetically constrained model [12]) but it is different from the law found in the hard-square lattice gas model [11]. This singular behaviour of D is in accordance with the prediction of MCT. From the behaviour of D and τ we obtain $D^{-1} \propto \tau$ and therefore, due to the proportionality of τ and η, where η is the viscosity, the Stokes–Einstein relation $D^{-1} \propto \eta$. The fact that the model does not capture the phenomenon of 'breakdown of Stokes–Einstein relation', usually observed in supercooled liquids, may be due to the fact that the model is overly simplified with respect to glassy liquids. Note however that the MCT does not capture this phenomenon either.

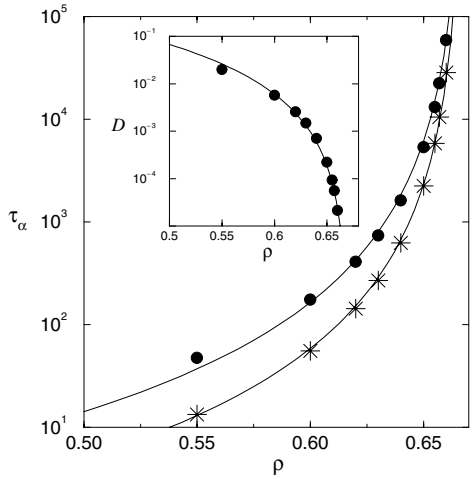

Figure 10. The relaxation times τ_α, obtained by the stretched exponential fits, as a function of density ρ. Solid circles: relaxation times of the self-part of density–density relaxations. Asterisks: relaxation times of the self-overlap. The solid curves are power law functions $\tau_\alpha = a(0.666 - \rho)^{-2.7}$, with $a = 0.115$ in the former case and $a = 0.04$ in the latter. Inset: the diffusion constant D as function of density ρ. The fitting function is a power law $D = 8(0.666 - \rho)^{2.7}$.

5. Conclusions

We have proposed a two-dimensional geometrical model, based on the concept of geometrical frustration which is generated by the particle shape. This model has neither quenched disorder nor kinetic constraints.

A self-overlap parameter $\langle q(t)\rangle$ has been defined which takes into account the orientation of particles, and the corresponding dynamical non-linear susceptibility has been studied. It has been found that the self-overlap can be fitted at long times by a stretched exponential function, with an exponent β decreasing until the arm percolation is reached, and constant for higher densities. The α-relaxation time found from the fit diverges at the maximum density $\rho = 2/3$, with an exponent $\gamma = 2.7$. For high density, near to the maximum density and structural arrest of the system, the self-overlap parameter develops a two-step relaxation, due to the different times of the rotational and translational dynamics.

The dynamical susceptibility shows a peak at some characteristic time, which seems to diverge at the maximum density. This gives evidence of long-lived dynamical structures with a growing length and relaxation time, as found in molecular dynamics simulations of Lennard-Jones liquids.

Similar results have been found for the self-part of density–density relaxation functions, but in this case there is only one step in the relaxation, due to the absence of the rotational degrees of freedom in the definition of $F_{\boldsymbol{k}}^s(t)$.

Acknowledgments

This work was supported in part by the European TMR Network—Fractals (contract no FMRXCT980183), MURST-PRIN-2000 and INFMPRA(HOP). We acknowledge the allocation of computer resources from INFM Progetto Calcolo Parallelo. ADS acknowledges support from a postdoctoral grant from the European TMR Network—Fractals.

References

[1] See, e.g., Mezei F and Murani A P 1979 *J. Magn. Magn. Mater.* **14** 211
Meyer C, Hartmann-Boutron F, Gross Y and Campbell I A 1985 *J. Magn. Magn. Mater.* **46** 254
[2] Kohlrausch R 1854 *Ann. Phys., Lpz.* **91** 179
Williams G and Watts D C 1970 *Trans. Faraday Soc.* **66** 80
[3] Randeria M, Sethna J P and Palmer R G 1985 *Phys. Rev. Lett.* **54** 1321
Cesi F, Maes C and Martinelli F 1997 *Commun. Math. Phys.* **188** 135
Franzese G and Coniglio A 1998 *Phys. Rev.* E **58** 2753
[4] Fierro A, de Candia A and Coniglio A 1997 *Phys. Rev.* E **56** 4990
[5] Fortuin C M and Kasteleyn P W 1972 *Physica* **57** 536
Coniglio A and Klein W 1980 *J. Phys. A: Math. Gen.* **12** 2775
[6] Fierro A, Franzese G, de Candia A and Coniglio A 1999 *Phys. Rev.* E **59** 60
[7] Doliwa B and Heuer A 1998 *Phys. Rev. Lett.* **80** 4915
Donati C, Glotzer S C and Poole P H 1999 *Phys. Rev. Lett.* **82** 5064
Benneman C, Donati C, Baschnagel J and Glotzer S C 1999 *Nature* **399** 246
[8] Donati C, Franz S, Parisi G and Glotzer S C 1999 *Preprint* cond-mat/9905433
[9] Coniglio A 1994 *Nuovo Cimento* D **16** 1027
Coniglio A 1997 *Proc. Int. School of Physics 'Enrico Fermi' (Course CXXXIV)* (Amsterdam: IOS Press)
[10] Fierro A, de Candia A and Coniglio A 2000 *Phys. Rev.* E **62** 7715
[11] Gaunt D S and Fisher M E 1966 *J. Chem. Phys.* **45** 2482
Ertel W, Froböse K and Jäckle J 1988 *J. Chem. Phys.* **88** 5027
Froböse K 1989 *J. Stat. Phys.* **55** 1285
Jäckle J, Froböse K and Knödler D 1991 *J. Stat. Phys.* **63** 249
[12] Fredrickson G H and Andersen H C 1984 *Phys. Rev. Lett.* **53** 1244
Fredrickson G H and Andersen H C 1985 *J. Chem. Phys.* **83** 5822
Kob W and Andersen H C 1993 *Phys. Rev.* E **48** 4364
[13] Graham I S, Pihé L and Grant M 1997 *Phys. Rev.* E **55** 2132
[14] Nicodemi M and Coniglio A 1998 *Phys. Rev.* E **57** R39
[15] Barrat A, Kurchan J, Loreto V and Sellitto M 2001 *Phys. Rev.* E **63** 51 301
[16] Caglioti E, Loreto V, Herrmann H J and Nicodemi M 1997 *Phys. Rev. Lett.* **79** 1575
[17] Stauffer D and Aharoni A 1994 *Introduction to Percolation Theory* (London: Taylor and Francis)
[18] Götze W 1991 *Liquids, Freezing and Glass Transition* ed J P Hansen, D Levesque and P Zinn-Justin (Amsterdam: Elsevier)
Götze W and Sjogren L 1992 *Rep. Prog. Phys.* **55** 241